Int. J. Electrochem. Sci., 10 **(2015)** 9466 - 9474

International Journal of
ELECTROCHEMICAL
SCIENCE
www.electrochemsci.org

Short Communication

Hierarchical Nanorod/Nanoflower TiO_2 Photoanode for Natural Dye-Sensitized Solar Cells

Tae Young Kim[1], Seok Jae Kim[2], Eun Mi Han[3], Jung Hun Kim[4], Jae Wook Lee[4], Kyung Hee Park[5,]*

[1]Department of Environmental and Energy Engineering, Chonnam National University, Gwangju 500-757, Korea
[2]Department of Advanced Chemicals & Engineering, Chonnam National University, Gwangju 500-757, Korea
[3]Department of Applied Chemical Engineering, Chonnam National University, Gwangju, 500-757, Korea
[4]Department of Chemical and Biochemical Engineering, Chosun University, Gwangju 501-759, Korea
[5]The Research Institute of Advanced Engineering Technology, Chosun University, Gwangju 501-759, Korea
[*]E-mail: see0936@chosun.ac.kr (K.H.Park)

Received: 17 May 2015 / *Accepted:* 27 July 2015 / *Published:* 30 September 2015

Different morphologies of rutile TiO_2 from microsphere, nanowire, and hierarchical nanorod/nanoflowers are successfully fabricated via hydrothermal reactions of titanium tetraisopropoxide and hydrochloric acid. Dye-sensitized solar cells (DSSCs) were assembled using natural *gardenia yellow* dyes extracted from *Gardenia Jasminoide Ellis* as a sensitizer. In this work, we studied the adsorption characteristics for harvesting sunlight and the electrochemical behavior for electron transfer in gardenia yellow DSSC using different morphologies TiO_2 photoanode. The DSSC based on the hierarchical rutile TiO_2 nanorod/nanoflower photoelectrode shows an energy conversion efficiency of 0.85% accompanying a short-circuit current density of 2.11 mA cm^{-2}, an open-circuit voltage of 0.63 V and fill factor of 0.64, which is higher than that of microsphere (0.71%), nanowires (0.61%). The enhancement of short-circuit current density and energy conversion efficiency for the hierarchical nanorod/nanoflower-based DSSC compared to other structures is mainly contributed to the larger dye loading, higher light scattering ability, and faster electron transport.

Keywords: Gardenia yellow, TiO_2 Morphology, Dye-sensitized solar cells, Adsorption properties

1. INTRODUCTION

Dye-sensitized solar cell (DSSC) has been discovered as a great promising device for generation of renewable energy because of low-cost manufacture process and its imposing efficiency [1,2]. A dye-sensitized solar cell is usually composed of a dye-adsorpted nanocrystalline porous

semiconductor electrode, a novel metal counter electrode, and a redox electrolyte mediating electron transfer processes occurring in the cell [3].

Among the components, the TiO_2 photoelectrode has been widely studied because it plays important roles in the DSSC, such as the support of dye and the pathway of electrons generated from dyes. It is now well-accepted that a high-efficiency photoelectrode for DSSCs requires not only a high surface area for large dye loading but also a tailored microstructure for light harvesting and fast electron transport [4-6].

The prominent wet-chemical synthesis-methods to prepare TiO_2 nanostructure are sol–gel [7,8] and hydrothermal [9]. Many studies have been made for controlling the morphology of TiO_2 using the effects of temperature, Ti-containing precursor, acid and reaction concentration based hydrothermal method [10].

The one-dimensional (1D) TiO_2 nanorod and nanowires can improve electron transport by providing direct electrical pathways but this nanostructure may have a low amount of dye adsorption and light scattering, because of the large number of gaps existing among the rods and wires [11]. However, the hierarchical nanorod/nanoflower-based DSSC compared to other nanostructures is mainly attributed to the larger dye loading, superior light scattering ability, and/or faster electron transport and longer electron lifetime.

Owing to the high cost of ruthenium complexes and low availability of those noble metals as a dye, attention has been looked for cheaper, simpler, and safer sensitizers [12]. Natural pigments, including betalains, chlorophyll, flavonoids and carotenoids, can fulfill those requirements, and sensitization on TiO_2 porous films by natural pigments has been reported. The natural dyes are readily available, easy to extract, of less cost, and environmentally friendly [13]. The gardenia yellow was usually extracted from gardenia jasminoides by extraction methods with water, alcohol and ultrasonication [14].

In this wok, three different morphologies of TiO_2 structures (microspheres, nanowires, nanorod/ nanoflowers) were selected as the photoanode materials for natural DSSC application. Systematic studies on the influence of the TiO_2 morphologies on the adsorption and photovoltaic performance of natural dyes have not yet been investigated so far. Therefore, we investigated the absorption spectra of gardenia yellow under different TiO_2 morphologies. Adsorption kinetics data were obtained and analyzed by employing a pseudo-second-order model.

2. EXPERIMENT

Titanium isopropoxide ($Ti[OCH(CH_3)_2]_4$, 97%), hydrochloric acid (HCl, 37 wt%), and isopropyl alcohol were purchased from Sigma-Aldrich (Sigma-Aldrich Korea) and used as received. All chemicals were of analytical grade and used as received without further purification. Deionized water was used throughout this study. The dilution of HCl was chosen as a control to tailor precursor hydrolysis rate which depends with the change in volume (v/v) proportion of water in HCl. Dilution of HCl with water as 3:7, 5:5, and 7:3, respectively was obtained and separately 40 ml of differently diluted solutions of HCl were missed with 1ml of titanium isopropoxide. Cleaned fluorine doped tin

oxide (FTO) substrates were placed in different solutions and these were placed in the autoclave. The autoclave was set at 180 °C for 3 h. For, simultaneous growth of TiO_2 as nanorod/nanoflower like structure in a hydrothermal synthesis, the reaction solutions described above was placed in a Teflon-lined stainless steel autoclave. After the reaction was completed at desired temperatures and times, the autoclave was allowed to cool to room temperature. The TiO_2 nano-structures grown on FTO substrates at different types of conditions used as described above were collected, washed with deionized water and absolute ethanol several times, and then dried in vacuum at 70 ^oC for 12 h before the use [15].

The preparation of electrode, electrolyte and assembly of DSSCs was likewise described in our previous works [16]. The film surface morphology and thickness were characterized by field emission scanning electron microscopy (FE-SEM, Hitachi, S-4700). The prepared samples were analyzed by UV-Vis spectrophotometer (Shimadzu UV-1601A, Japan) and electrochemical workstation (CHI660A, USA). The photovoltaic properties were investigated by measuring the J-V characteristics under the irradiation of white light from a 200 W Xenon lamp (McScience, Korea).

3. RESULTS AND DISCUSSION

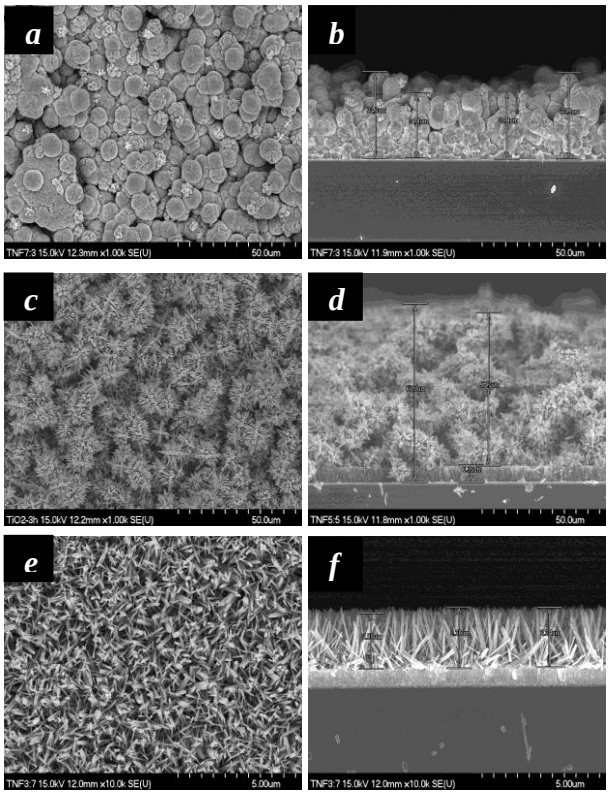

Figure 1. FE-SEM images of TiO_2 structure grown on FTO substrates. Top and cross sectional view of nano-structures grown at different HCl to water ratio (a and b) 3:7; (c and d) 5:5; (e and f) 7:3.

Figure 1 shows scanning electron microscopy (SEM) images of the TiO_2 films prepared at various HCl to water ratio. The effects of dilution of HCl solutions ((a)-(f)) on controlling the growth of TiO_2 nanostructures as films on FTO substrates was optimized at 3hrs of reaction time and 180 ^oC temperatures. At lower concentration of HCl (a and b), 3D round ball like TiO_2 structures was observed (thickness; 25~32 μm). Gradual increase in HCl concentration of H_2O (c and d) showed transformation of 3D round ball structure to nanorod/nanoflower structure (thickness of rod; 6.4 μm, flower; 57.7 μm). Further increase in HCl condition (e and f) shows wire like TiO_2 structure (thickness; 2.3 μm).

Adsorption isotherm of dye molecular is very important in the photoelectrode of DSSCs. The adsorption characteristics of the *GY* on TiO_2 thin film in terms of dilution of HCl with water were evaluated on the basis of adsorption equilibrium and kinetic studies. The adsorption capacity of *GY* on TiO_2 thin film was analyzing by direct measurement of the amount of dye adsorbed on the adsorbent. The adsorption amount of *GY* on TiO_2 thin film with mole ratio of water and HCl was in order of 5:5 > 7:3 > 3:7 as shown in figure 2. The difference of dye uptakes with mole ratio of water and HCl is attributed to surface morphologies of the TiO_2 thin film. As can be seen in figure 1, the morphologies of TiO_2 grown on FTO substrates with mole ratio of water and HCl were very different as microspheres (a), nanowires (b) and hierarchical nanorod/nanowires.

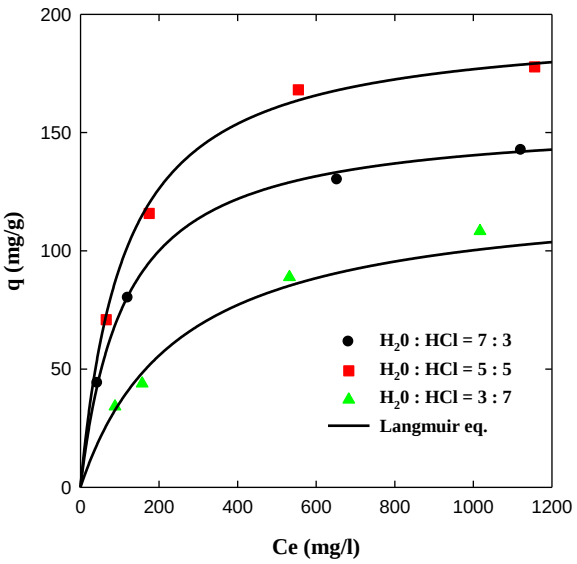

Figure 2. Adsorption isotherms of *Gardenia yellow* on TiO_2 thin film with mole ratio of H_2O and HCl (298 K).

The adsorption capacity of *GY* on TiO_2 thin film with ratio of water and HCl was 156.18 (for 7:3), 196.43 (for 5:5), and 125.3 mg/g (for 3:7). The Langmuir isotherm model was fitted to describe the adsorption equilibrium. The isotherm equation is shown below [17]:

$$q = \frac{q_m b c_e}{1 + b c_e} \qquad (1)$$

where c_e is the supernatant concentration at equilibrium (mg/l), b the Langmuir affinity constant and q_m the maximum adsorption capacity of the material (mg/g) assuming a monolayer of adsorbate was taken up by the adsorbent.

To find the parameters for the adsorption isotherm, the linear least square method and a pattern search algorithm were used. The value of the mean percentage error has been used as a test criterion for the fit of the correlations. The mean percentage deviation between the experimental and predicted values was obtained using equation 2.

$$error(\%) = \frac{100}{N}\sum_{k=1}^{N}\left[\frac{\left|q_{\exp,k} - q_{mol,k}\right|}{q_{\exp,k}}\right] \qquad (2)$$

where $q_{cal,\,k}$ is each value of q predicted by the fitted model and $q_{exp,\,k}$ each value of q measured experimentally and N the number of experiments performed. The parameters and average percentage differences between the measured and calculated values for the adsorption of *GY* on TiO_2 thin film with mole ratio of water and HCl are given in Table 1. The Langmuir model fitted well the experimental data of *GY* (Fig. 2), which means that the q fit by the isotherm model was close to the q measured experimentally.

Table 1. Langmuir isotherm constants of *GY* on TiO_2 thin film with mole ratio of H_2O and HCl (298 K).

Isotherm type	Parameters	H_2O:HCl (7 : 3)	H_2O:HCl (5 : 5)	H_2O:HCl (3 : 7)
Langmuir	q_m	156.18	196.43	125.3
	b	0.009	0.009	0.004
	Error (%)	1.67	2.09	6.32

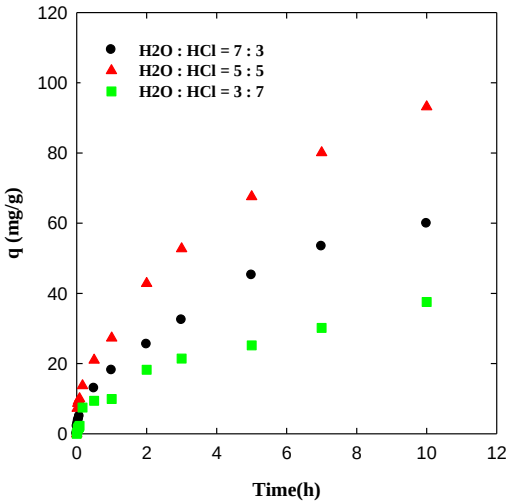

Figure 3. **V**ariation of adsorbed amounts of *GY* on TiO_2 thin film with mole ratio of H_2O and HCl (Co : 250 mg/l, 298 K).

Figure 3 shows the variation of adsorbed amounts of *GY* on TiO_2 thin film in terms of adsorption time with mole ratio of H_2O and HCl. Adsorption amount of GY on TiO_2 thin film increased with increasing adsorption time. When adsorption time is 10 h, the adsorption amount of *GY* on TiO_2 thin film with mole ratio of H_2O and HCl was 59.85 (for 7:3), 93.13 (for 5:5), and 35.55 mg/g (for 3:7).

The differences in the rates of adsorption on TiO_2 thin film were primarily attributable to the differences in the equilibrium adsorption capacities of the adsorbent (shown in figure 2).

Table 2. Kinetic parameters of *GY* adsorption on TiO_2 film

Concentration [mg/l]	Pseudo-second order		
	$k_2 \times 10^{-5}$ [g/mg/min]	q_e [mg/g]	R^2
1000	6.866	553.84	0.993
500	9.141	359.21	0.991
250	16.37	183.59	0.995

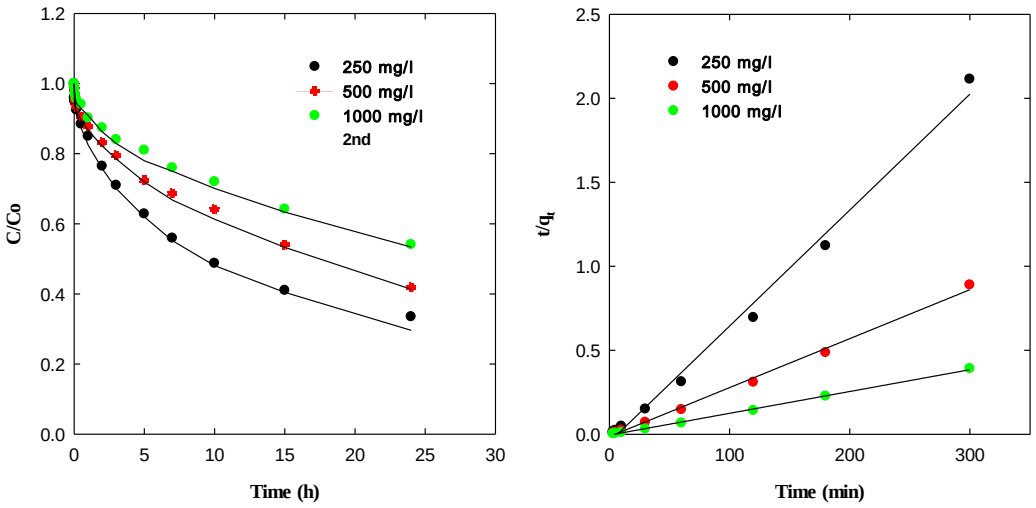

Figure 4. Concentration decay curves (left) and linearized pseudo-second order kinetic model (right) of *GY* on TiO_2 thin film (H_2O:HCl = 5:5, 298 K).

The adsorption kinetics can predict the rate of adsorption of *GY* on the TiO_2 thin film from the dye solution. Figure 4 shows the concentration decay curves of *GY* on the TiO_2 thin film prepared 5:5 mole ratios of H_2O and HCl. The initial concentrations of *GY* were 1000, 500, 250 mg/L, respectively, and the temperature was 298 K. As can be seen in this figure 4, the adsorption rate increased with decreasing initial concentration of *GY*. The pseudo-second-order model shows satisfactory prediction

of the concentration decay curves. The kinetic data were analyzed with the Pseudo-second-order model. The second order kinetic model is expressed as [18]:

$$\frac{t}{q_t} = \frac{1}{k_{2,ad} q^2_{eq}} + \frac{1}{q_{eq}} t \qquad (3)$$

where k_2 is the rate constant of the pseudo- second-order kinetic model (g/mg/min).

The rate parameters k_2 and q_e can be directly obtained from the intercept and slope of a plot of t/q_t versus t, as shown in Fig. 4. Table 2 shows the adsorption kinetics parameters of the pseudo second-order model of *GY* on the TiO_2 thin film. The determined rate constants of q_e and k_2 were in the ranges 183 - 553 mg/g and 6.866 - 16.37 g/mg/min, respectively. The correlation coefficients (R^2) of the pseudo second-order model for the linear plots were very similar to 1. This result implies that the adsorption kinetics was successfully described by the pseudo-second-order model.

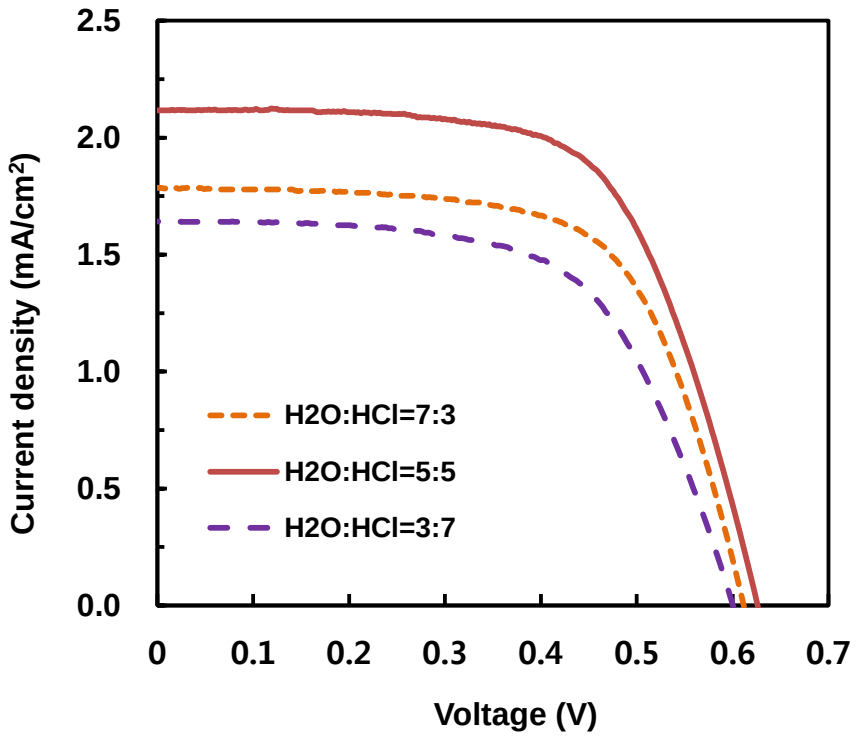

Figure 5. Photocurrent-voltage curves of GY based DSSC with mole ratio of H_2O and HCl.

The hydrothermally synthesized TiO_2 microsphere (H_2O:HCl = 7:3) based DSSC produced power conversion efficiency (η%) of 0.71% with short circuit current density (J_{sc}) 1.79 mA cm^{-2}, open circuit voltage (Voc) 0.61 V and fill factor (FF) 66%. The nanorod/nanoflower sample (H_2O:HCl = 5:5) shows η of 0.85% (J_{sc} = 2.11 mA cm^{-2}, V_{oc} = 0.63 V, FF = 64%). It is also noted that the Voc of the nanoflower sample is increased; which may be due to the change in Fermi level of the

nanorod/nanoflower sample prepared at 0.3 pH, 180 ^{o}C and 3 h of reaction time. IV response of nanowire TiO_2 based DSSC with ratio of water and HCl (3:7) showed decrease in DSSC efficiency (η =0.61%).

4. CONCLUSIONS

We successfully fabricated the microsphere, nanowire, and hierarchical nanorod/nanoflowers via hydrothermal reactions depending on the different contents of HCl and water for dye-sensitized solar cells. Adsorption isotherm data were fitted with the Langmuir isotherm and the adsorption kinetic data were accurately described by the pseudo-second-order model. The hierarchical rutile TiO_2 nanorod/nanoflower photoelectrode (H_2O:HCl = 5:5) shows an overall light-to-electricity conversion efficiency of 0.85% accompanying a short-circuit current density of 2.11 mA cm^{-2}, an open-circuit voltage of 0.63 V and fill factor of 0.64, which is higher than that of microsphere (0.71%), nanowires (0.61%). The systematic studies of adsorption equilibrium and kinetics obtained in this work could be widely applied to the study of other natural DSSCs.

ACKNOWLEDGMENT
This work was supported by the Human Resources Development program(No. 20134010200560) of the Korea Institute of Energy Technology Evaluation and Planning(KETEP) grant funded by the Korea government Ministry of Trade, Industry and Energy

References

1. D.S. Hwang, S.M. Jo, D.Y. Kim, V. Armel, D. R. MacFarlane and S.Y. Jang, *ACS Appl. Mater. Interfaces* 3 (5) (2011) 1521.
2. H.Y. Chen, D.B. Kuang and C.Y. Su, *J. Mater. Chem.* 22 (2012) 15475.
3. H. Xu, X. Tao, D.T. Wang, Y.Z. Zheng and J.F. Chen, *Electrochim. Acta* 55 (2010) 2280.
4. Q. Zhang and G. Cao, *Nano Today* 6 (2011) 91.
5. Y.Z. Zheng, H. Ding, Y. Liu, X. Tao, G. Cao and J.F. Chen, *J. Power Sources* 254 (2014) 153.
6. J.W. Lee, T.Y. Kim, H.S. Ko, S. Han, S.H. Lee and K.H. Park, *Spectrochim. Acta Part A: Mol. Biomol. Spectrosc.* 126 (2014) 76.
7. Y. Wang, Y. He, Q. Lai and M. Fan, *J. Environ. Sci.* 26 (2014) 2139.
8. F. Xu, Y. Wu, X. Zhang, Z. Gao and K. Jiang, *Micro & Nano Letters* 7 (2012) 826.
9. S.S. Mali, C. A. Betty, P.N. Bhosale, R.S. Devan, Y.R. Ma, S.S. Kolekar and P.S. Patil, *CrystEngComm* 14 (2012) 1920.
10. H.E. Wang, Z.C. Chen, Y.H. Leung, C. Luan, C. Liu, Y. Tang, C. Yan, W. Zhang, J.A. Zapien, L. Bello and S.T. Lee, *Appl. Phys. Lett.* 96 (2010) 263104.
11. M. Lv, D. Zheng, M. Ye, L. Sun, J. Xiao, W. Guo and C. Lin, *Nanoscale* 4 (2012), 5872.
12. N. Li, N. Pan, D. Li and S. Lin, *Int. J. Photoenergy* (2013) 598753.
13. M.R. Narayan, Renew. Sust. Energy Rev. 16 (2012) 208.
14. O.O. Kwon, E.J. Kim, J.H. Lee, T.Y. Kim, K.H. Park, S.Y. Kim, H.J. Suh, H.J. Lee and J.W. Lee, *Spectrochim. Acta Part A: Mol. Biomol. Spectrosc.* 136 (2015) 1460.
15. K.H. Park and M. Dhayal, *Electrochem. Commun.* 49 (2014) 47.

16. K.H. Park, T.Y. Kim, J.Y. Park, E.M. Jin, S.H. Yim, D.Y. Choi and J.W. Lee, *Dyes Pigment.* 96 (2013) 595.
17. N.T.R.N. Kumara, N. Hamdan, M.I. Petra, K. u. Tennakoon and P. Ekanayake *J. Chem.* 2014 (2014) Article ID 468975.
18. Y.S. Ho and G. McKay, *Process Biochem.* 34 (1999) 451.